COMPUTER STUDIES OF BEAM DYNAMICS IN A PROTON LINEAR ACCELERATOR WITH SPACE CHARGE

M. MARTINI

ing. C. Olivetti S.p.A,† Italy

AND

M. PROMÉ

Centre d'Etudes Nucléaires de Saclay, France

Two computer programs written for investigating space-charge effects in proton linear accelerators are presented. Both use the dynamics equations derived by Drs. P. Lapostolle and B. Schnizer: the way these equations have been practically treated is explained. Details are given on the two programs: the first one is based on a particle to particle interaction, while the second one benefits from a continuous equivalent distribution. Results given by both programs are compared and contrasted to Dr. R. Chasman's previous results. As an application, the problem of the influence of injection energy on linac performance is partially treated.

1. INTRODUCTION

Present-day proton linacs can accelerate such high-intensity currents that it is necessary to include space charge effects in beam dynamics problems. Following the way opened by Dr. Chasman,[1,2] it was decided at CERN and at CEN Saclay to study and to set up, in a joint effort, some means of computing particle dynamics taking into account space-charge forces. Two main goals were aimed at: (i) anticipating the beam behaviour in an existing accelerator (tank 1 of the CERN PS injector), and (ii) understanding the phenomena observed in all high-intensity linacs, namely the beam emittance blow-up in passing through the accelerator. An article, completely dedicated to this latter item, will soon be submitted to this journal.

In this paper we shall present the ideas on which are based two computer programs, MAPRO 1 and MAPRO 2, written as a result of the above-mentioned collaboration. Some of the results and of the preliminary conclusions which can be drawn by running the programs also are given.

2. DYNAMICS WITHOUT SPACE CHARGE

2.1. *Theoretical Equations*

At the time when it was decided to include space-charge effects in the computation of particle trajec-

† Formerly at CERN.

tories, a new set of dynamics equations was available. In the first computer programs, the longitudinal and the radial particle motion were treated separately. Longitudinally the set of equations used was:

$$\frac{dW}{dz} = eET\cos\phi$$

$$\frac{d\phi}{dz} = \frac{2\pi}{\lambda}\left(\frac{1}{\beta} - \frac{1}{\beta_s}\right)$$

where the notation is the usual one.

Radially, the action of the force continuously deflecting the particle across the gap was replaced by one or several impulses at some discrete points. Then it was realized that, if the dependence of the transit time factor on the particle velocity was to be taken into account, a term had to be added in the ϕ equation in order to satisfy Liouville's theorem on the axis.[3]

It was also understood that simple radial impulses were not sufficient and that a radial displacement had to be added.[4]

Finally it was strongly felt that the opportunity should be exploited, in dynamics computations, of the precise knowledge of the electromagnetic field in linac cavities yielded by new powerful computer programs such as MESSYMESH[5] and CLAS.[6]

The new equations, due to Drs. P. Lapostolle and B. Schnizer,[7] have the advantage of being rigorous thanks to the use of a certain number of

parameters (basically field integrals across the gap) calculated directly by CLAS.

By using these equations, one substitutes for the 'true' trajectory an 'equivalent' one, discontinuous, which coincides with the true trajectory at the entrance (index 1), at the midpoint (no index) and at the output of the gap (index 2). As shown in Fig. 1, the particle, in the fictitious motion,
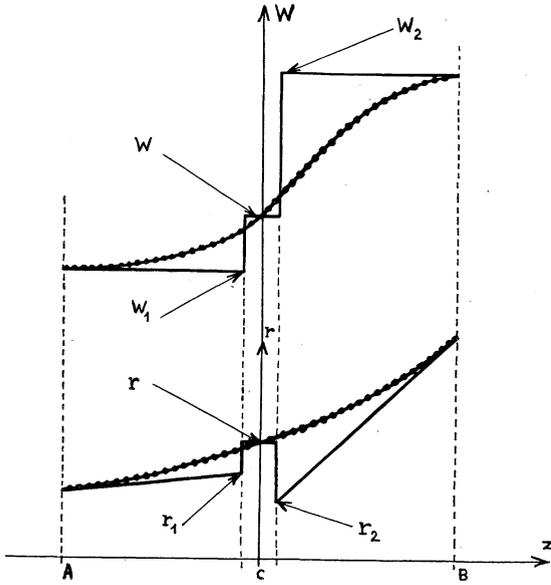

FIG. 1. True and equivalent variations of W and r when crossing a gap. AB: accelerating gap; C: center of the gap; ————: equivalent variation; –··–··–··–: true variation.

drifts, at constant speed, from the end of a quadrupole to the middle of the gap; undergoes a discontinuity in its six phase-space coordinates and drifts again to the input of the next quadrupole.

As a matter of fact, Lapostolle and Schnizer's equations proceed in two steps: a first set of equations gives the equivalent change in coordinates across the whole gap assuming that the value of these same coordinates in the middle of the gap known; another set of equations allows one to calculate effectively the latter by giving the equivalent change of coordinates across the first half of the gap.

The equations exist in a relativistic form, but we shall give here the nonrelativistic sets, the only ones

of interest throughout this paper:

$$W_2 - W_1 = eV_0\,T_0\,I_0\cos\phi + eV_0\frac{\mathrm{d}}{\mathrm{d}k}(T_0\,kI_1)r'\sin\phi$$

$$\phi_2 - \phi_1 = \alpha k\frac{\mathrm{d}}{\mathrm{d}k}(T_0\,I_0)\sin\phi$$
$$\qquad\qquad -\alpha k\frac{\mathrm{d}^2}{\mathrm{d}k^2}(T_0\,kI_1)r'\cos\phi$$

$$r_2' - r_1' = -\alpha T_0\,I_1\sin\phi$$
$$\qquad\qquad +\alpha\left[\frac{\mathrm{d}}{\mathrm{d}k}(T_0\,kI_1') - T_0\,I_0\right]r'\cos\phi$$

$$r_2 - r_1 = -\alpha\frac{\mathrm{d}}{\mathrm{d}k}(T_0\,I_1)\cos\phi$$
$$\qquad\qquad -\alpha\left[\frac{\mathrm{d}^2}{\mathrm{d}k^2}(T_0\,kI_1') - \frac{\mathrm{d}}{\mathrm{d}k}(T_0\,I_0)\right]r'\sin\phi$$

$$W - W_1 = \frac{W_2 - W_1}{2} + \frac{eV_0}{2}\left[S_l\sin\phi - \frac{\mathrm{d}}{\mathrm{d}k}\frac{\partial S_l}{\partial r}r'\cos\phi\right]$$

$$\phi - \phi_1 = \frac{\phi_2 - \phi_1}{2}$$
$$\qquad\quad -\frac{\alpha k}{2}\left[\frac{\mathrm{d}S_l}{\mathrm{d}k}\cos\phi + \frac{\mathrm{d}^2}{\mathrm{d}k^2}\frac{\partial S_l}{\partial r}r'\sin\phi\right]$$

$$r' - r_1' = \frac{r_2' - r_1'}{2}$$
$$\qquad\quad -\frac{\alpha}{2}\left[S_r\cos\phi + \left(\frac{\mathrm{d}}{\mathrm{d}k}\frac{\partial S_r}{\partial r} + S_l\right)r'\sin\phi\right]$$

$$r - r_1 = \frac{r_2 - r_1}{2}$$
$$\qquad\quad +\frac{\alpha}{2}\left[\frac{\mathrm{d}S_r}{\mathrm{d}k}\sin\phi - \left(\frac{\mathrm{d}^2}{\mathrm{d}k^2}\frac{\partial S_r}{\partial r} + \frac{\mathrm{d}S_l}{\mathrm{d}k}\right)r'\cos\phi\right]$$

Besides: T_0, transit time factor on the axis, is a function of k given by

$$T_0(k) = \frac{2}{L}\int_0^{L/2} E_z(z,0)\cos kz\,\mathrm{d}z, \qquad k = \frac{\omega}{\beta c}$$

where ω is the high frequency pulsation,

βc is the longitudinal velocity of the particle,

L is the cell length,

E_z is the longitudinal electric field on the axis.

The argument of the Bessel functions I_0 and I_1 is kr. S_l is a function of k and r given by:

$$S_l(k, r) = \frac{2}{L} \int_0^{L/2} E_z(z, r) \sin kz \, dz$$

where $E_z(z, r)$ is the longitudinal electric field at the radius r; the power expansion of S_l is limited to two terms:

$$S_l(k, r) = S_0(k) + S_1(k) r^2$$

S_r also is a function of k and r

$$S_r(k, r) = \frac{2}{L} \int_0^{L/2} E_r(z, r) \cos kz \, dz$$

where $E_r(z, r)$ is the radial electric field at the radius r; the power expansion of S_r is limited to one term:

$$S_r(k, r) = r S'(k)$$

$$\alpha = \frac{e V_0}{2W}$$

where V_0 is the rf peak voltage in the accelerating interval.

2.2. Practical Equations

The dynamics equations, in the form given in the preceding section, cannot be easily used in practice for two main reasons: (i) they are not solved with respect to the desired quantities; (ii) they make use of differentials in T_0, S_r and S_l which can be profitably replaced by introducing some field integrals.

In what follows we shall set:

$$T_0 = \frac{2}{L} \int_0^{L/2} E_z(z, 0) \cos \frac{2\pi z}{L} \, dz$$

$$T_1 = k \frac{dT_0}{dk} = -\frac{2}{L} \frac{2\pi}{L} \int_0^{L/2} E_z(z, 0) z \sin \frac{2\pi z}{L} \, dz$$

$$T_2 = k^2 \frac{d^2 T_0}{dk^2} = -\frac{2}{L} \left(\frac{2\pi}{L}\right)^2 \int_0^{L/2} E_z(z, 0) z^2 \cos \frac{2\pi z}{L} \, dz$$

$$S' = \frac{2}{L} \int_0^{L/2} \frac{E_r(z, r)}{r} \cos \frac{2\pi z}{L} \, dz$$

$$\bar{S} = k \frac{dS'}{dk} = -\frac{2}{L} \frac{2\pi}{L} \int_0^{L/2} \frac{E_r(z, r)}{r} z \sin \frac{2\pi z}{L} \, dz$$

$$\bar{\bar{S}} = k^2 \frac{d^2 S'}{dk^2} = -\frac{2}{L} \left(\frac{2\pi}{L}\right)^2 \int_0^{L/2} \frac{E_r(z, r)}{r} z^2 \cos \frac{2\pi z}{L} \, dz$$

$$S_0 = \frac{2}{L} \int_0^{L/2} E_z(z, 0) \sin \frac{2\pi z}{L} \, dz$$

$$\bar{S}_0 = k \frac{dS_0}{dk} = \frac{2}{L} \frac{2\pi}{L} \int_0^{L/2} E_z(z, 0) z \cos \frac{2\pi z}{L} \, dz$$

S_1 and $\bar{S}_1 = k(dS_1/dk)$ are calculated from values of S_l and $\bar{S}_l$ off axis. All these coefficients are computed directly by CLAS. Also:

$I_1(kr)$ is approximated by $kr/2$.

$I_0(kr)$ is approximated by:

  (i) $1 + (k^2 r^2/4)$ in the equation in W and ϕ.
  (ii) 1 in the equation in r' and r.

After several algebraic manipulations, by neglecting higher order terms (energy gain in crossing the gap/kinetic energy), which is allowed since the theoretical starting equations apply in the same approximation, one obtains the following set of equations:

$$r = r_1 - \frac{e E_e L}{4W} \left\{ \left(\frac{T_0 + T_1}{2} \cos \phi_1 - \frac{\bar{S}}{k} \sin \phi_1 \right) r_1 \right.$$
$$\left. + \left[\frac{T_2}{2k} \sin \phi_1 + \left(\frac{\bar{S}}{k^2} + \frac{\bar{S}_0}{k} \right) \cos \phi_1 \right] r_1' \right\}$$

$$r' = r_1' - \frac{e E_e L}{4W} \left\{ \left[\left(\frac{T_0 - T_1}{2} \right) \cos \phi_1 \right. \right.$$
$$\left. + \left(\frac{\bar{S}}{k} + S_0 \right) \sin \phi_1 \right] r_1'$$
$$\left. + \left(\frac{T_0 k}{2} \sin \phi_1 + S' \cos \phi_1 \right) r_1 \right\}$$

$$r_2 = r_1 - \frac{e E_e L}{4W} \left\{ \left[(T_1 + T_0) + \frac{\Delta k}{k} (2T_1 + T_2) \right] r \cos \phi \right.$$
$$\left. + \frac{T_2}{k} \left(1 + \frac{\Delta k}{k} \right) r' \sin \phi \right\}$$

$$r_2' = r_1' + \frac{e E_e L}{4W} \left\{ -k \left[T_0 + \frac{\Delta k}{k} (T_1 + T_0) \right] r \sin \phi \right.$$
$$\left. + \left[T_1 - T_0 + \frac{\Delta k}{k} T_2 \right] r' \cos \phi \right\},$$

where E_e is the mean longitudinal electric field in the cell of length L

$$\frac{\Delta k}{k} = \frac{W_r - W}{m_0 c^2 \beta^2}$$

and W_r is the reference kinetic energy at which all the coefficients yielded by CLAS were calculated.

$$\phi = \phi_1 + \frac{eE_e L}{4W}(B_1 \sin\phi_1 - B_2 \cos\phi_1)$$

with

$$B_1 = T_1 + \frac{k^2 r^2}{2}\left(T_0 + \frac{T_1}{2}\right)$$
$$+ \frac{\Delta k}{k}\left[T_1 + T_2 + k^2 r^2\left(T_0 + \tfrac{5}{4}T_1 + \frac{T_2}{4}\right)\right]$$

$$B_2 = rr'\left[k\left(T_0 + 2T_1 + \frac{T_2}{2}\right)\right.$$
$$\left.+ \frac{\Delta k}{k}k(T_0 + 5T_1 + \tfrac{7}{2}T_2)\right] + \left(1 + \frac{\Delta k}{k}\right)(\bar{S}_0 + r^2 \bar{S}_1)$$

$$W = W_1 + \frac{eE_e L}{2}\left(A_3 + \frac{\Delta k}{k}A_2\right)$$

with

$$A_2 = \left[T_1 + \frac{k^2 r^2}{2}\left(T_0 + \frac{T_1}{2}\right)\right]\cos\phi$$
$$+ \left[k\left(T_0 + 2T_1 + \frac{T_2}{2}\right)rr' + \bar{S}_0 + r^2 \bar{S}_1\right]\sin\phi$$

$$A_3 = T_0\left(1 + \frac{k^2 r^2}{4}\right)\cos\phi$$
$$+ \left[k\left(T_0 + \frac{T_1}{2}\right)rr' + S_0 + r^2 S_1\right]\sin\phi$$

$$\phi_2 = \phi_1 + \frac{eE_e L}{2W}(B_3 \sin\phi - rr' B_4 \cos\phi)$$

with

$$B_3 = T_1\left(1 + \frac{k^2 r^2}{4}\right) + T_0\frac{k^2 r^2}{2} + \frac{\Delta k}{k}\left[T_2\left(1 + \frac{k^2 r^2}{4}\right)\right.$$
$$\left.+ T_1(1 + \tfrac{5}{4}k^2 r^2) + T_0 k^2 r^2\right]$$

$$B_4 = k\left(T_0 + 2T_1 + \frac{T_2}{2}\right) + \frac{\Delta k}{k}k(T_0 + 5T_1 + \tfrac{7}{2}T_2)$$

$$W_2 = W_1 + eE_e L(A_1 \cos\phi + rr' A_2 \sin\phi)$$

with

$$A_1 = T_0\left(1 + \frac{k^2 r^2}{4}\right) + \frac{\Delta k}{k}\left[T_1\left(1 + \frac{k^2 r^2}{4}\right) + T_0\frac{k^2 r^2}{2}\right]$$

$$A_2 = k\left(T_0 + \frac{T_1}{2}\right) + \frac{\Delta k}{k}k\left(T_0 + 2T_1 + \frac{T_2}{2}\right),$$

where

$$\frac{\Delta k}{k} = \frac{W_r - W}{m_0 c^2 \beta^2}$$

Concerning the quadrupoles, the equations used are the classical ones without taking into account fringing fields. Their effect in fact is somewhat important in beam transport systems where emittances can exhibit very eccentric shapes but can be neglected in a linac where emittance patterns are more nearly circular.[8] The particle coordinates are transferred through a quadrupole in two steps in order to have their midplane values available.

3. THE SPACE-CHARGE CALCULATION

3.1. *Preliminary Remarks*

In a real beam, each bunch is made of some 10^9 protons. The number of particles taken into account in numerical computations varies from a few hundreds to a few thousands; these computed particles are intended to follow trajectories which could have been effective trajectories of protons in the real beam; therefore these particles must be considered as a sort of superparticle, carrying a sort of supercharge, so that the repulsive force between two such superparticles is expressed by:

$$|\mathbf{F}| = \frac{1}{4\pi\varepsilon_0}\frac{I}{4Nf}\frac{e}{r^2},$$

where

I is the beam intensity,

f is the rf frequency,

$4N$ is the number of superparticles representing the total beam,

e is the proton charge.

This formula can be justified by saying that superparticles carrying $I/4Nf$ Coulomb each produce a field which is on average the same as the real field produced by protons in the real beam.

According to the general philosophy of these calculations, the space-charge action is taken into account by giving twice per cell an impulsive change

to the velocity of each particle of the beam. This is done in the middle of the drift tubes and in the center of the gaps. As the equations used are not relativistic, the magnetic field effect has been ignored.

To compute the space-charge forces, one needs to know the particle coordinates in the real space. This is done by interpreting $(\beta\lambda/2\pi)\phi$ as a longitudinal distance (implicit is a change of the independent variable from distance to time). In other words, from the knowledge of the instant of time (phase) at which each particle crosses a given section one derives the position in space of each particle at a given instant of time.

Then the equations become:

$$\Delta r' = g(r, r', W, \phi) + G(r, \phi)$$

$$\Delta W = h(r, r', W, \phi) + H(r, \phi)$$

where g and h are the functions given in Sec. 2 when the calculation refers to the center of the gap and are zero in the middle of quadrupoles.

G and H, for each particle, are a function of the position of all others and represent Coulomb interactions.

It can be easily shown that:†

$$G(r, \phi) = \frac{l}{m_0 c^2 \beta^2} [F_r(r, \phi) - r'F_z(r, \phi)]$$

$$H(r, \phi) = F_z(r, \phi)l$$

The problem is to evaluate F_r and F_z. The simplest method of summing up all terms in $1/r^2$ is catastrophic as everybody who has tried knows. In fact space-charge forces are calculated from the positions that the particles occupy in their motion without space charge. In this condition it can happen that two particles get extremely close to each other; the repulsive force becomes then enormous and one has a local blow-up of the beam. In practice these collisions keep on taking place during the whole calculation and condemn the method. (See Fig. 2.)

Several tricks have been devised to bypass the difficulty. In the frame of this type of particle-to-particle interaction method, the program MAPRO 1, which makes use of the so called 'cage method', was written.

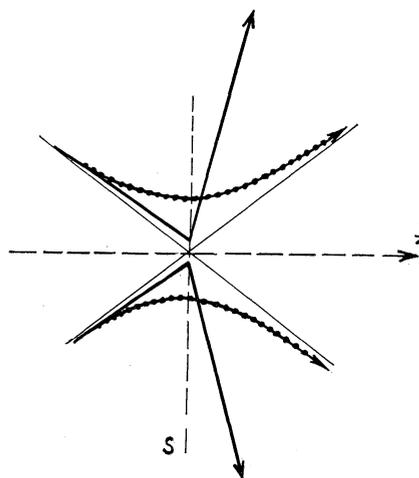† As in Sec. 2.1, r and r' stand for either x and dx/dz or y and dy/dz.

A5

FIG. 2. Accidental blow-up occurring in crude particle-to-particle interaction methods. -··-··-··-: true trajectory; ————: equivalent trajectory, calculated for zero current; space-charge effects are taken into account in Sec. S.

3.2. MAPRO 1

The cage method has already been used at CERN in the program BUNCH which computes the beam dynamics, with space charge, from the buncher to the linac.[9]

According to this method, the space volume around the bunch is enclosed in a cage, divided into a great number of small cubic (or, more generally, parallelepiped) cells, up to 27 000 in MAPRO 1. To calculate the electric field acting on one particle (field point) due to the presence of all the others (source points) one assumes that the field point coincides with a node of the three-dimensional grid and that the source points fall in the center of the elementary cubes. This corresponds to moving slightly, only for the sake of the space-charge calculation, all particles around their true position to make them 'fit' into the cage. In this manner, having put the source points at nodes of the grid, the number of possible space-charge forces becomes finite and they can be precalculated and stored in the computer memory. Thereafter, during the motion of the beam, the interaction between any two particles is obtained by selecting the convenient approximate force from the entries in the space-charge table. This can be done in a very fast manner, particularly if assembly language routines are used.

Also, as the minimum distance between two particles cannot be less than half a cell length (this is set so in the program even in the case of particles falling in the same cell), collisions are avoided. Clearly this method tends to underestimate space-charge effects; in practice, one sees that by varying the elementary cube side size around a value of about 0.5 mm the results do not change noticeably.

Unfortunately the cage method, though faster than other particle-to-particle interaction methods, is intrinsically time consuming (about 7.5 sec of CDC 6600 CPU time to calculate the complete interaction of 500 particles) and the time needed increases with the square of the number of representative particles used.

Therefore MAPRO 1 has essentially been used to compare results with those obtained with MAPRO 2 which is considerably faster and can treat up to 5000 particles.

3.3. MAPRO 2

This program is based on completely different principles. The basic idea is the following: one represents a bunch made up of, say, 10^9 protons by means of a few hundreds or thousands of representative particles. At the scale of these macro-particles the cloud of protons appears more like a continuous distribution and this is what is used in MAPRO 2. If one knows the analytical expression of the electric field generated by such a distribution a simple evaluation of this expression for each particle solves the problem. Note that (i) in this case the computer time needed will grow only linearly with the number of particles traced, and (ii) there is no risk of collisions inherent to the method.

Obviously one must choose a distribution which is sufficiently close to the real situation and such that one is capable of finding an analytical expression for its electrostatic field.

The distribution chosen for MAPRO 2 is of the type:

$$\chi(x, y, z) = \chi_0 \exp\left[-\frac{1}{2}\left(\frac{x^2}{a^2} + \frac{y^2}{b^2} + \frac{z^2}{c^2}\right)\right]$$

The isodensity surfaces are ellipsoids, and χ is the number of particles/meter^3. This distribution has no discontinuities and the charge density tends to zero far from origin: it cannot represent hollow

bunches but this is not a serious limitation in practice.

The choice of a, b, c and χ_0 can be made such that the equivalent distribution maintains some of the properties of the original one. The criterion adopted was to equate the lower order momenta. As the N particles traced are representative in fact of four times as many (one takes advantage, in MAPRO 2 as well as in MAPRO 1, of the existing symmetry with respect to x and y to fill in initially only the $x, y > 0$ portion of the beam), the zero and second-order momenta of the real distribution are:

$$4N, \quad 4\sum_1^N x_i^2, \quad 4\sum_i^N y^2, \quad 4\sum_i^N z_i^2$$

where z_i is the longitudinal barycentric coordinate. The same momenta for the equivalent distribution are:

$$\iiint \chi \, dx \, dy \, dz = (2\pi)^{3/2} abc\chi_0$$

$$\iiint x^2\chi \, dx \, dy \, dz = (2\pi)^{3/2} a^3 bc\chi_0$$

$$\iiint y^2\chi \, dx \, dy \, dz = (2\pi)^{3/2} ab^3 c\chi_0$$

$$\iiint z^2\chi \, dx \, dy \, dz = (2\pi)^{3/2} abc^3\chi_0$$

with the triple integrals extended to the whole space. Solving for the desired quantities, one finds:

$$a^2 = \frac{\sum_i^N x_i^2}{N} \qquad b^2 = \frac{\sum_i^N y_i^2}{N} \qquad c^2 = \frac{\sum_i^N z_i^2}{N}$$

$$\chi_0 = \frac{4}{(2\pi)^{3/2}} \frac{N}{abc}$$

The next step is now to calculate the electric field. The following can be proved:[10]

(i) given a three-dimensional charge distribution such that the density is constant over ellipsoids:

$$\frac{x^2}{a^2} + \frac{y^2}{b^2} + \frac{z^2}{c^2} = u^2$$

then the distribution depends only on u, i.e., $\chi = \chi(u)$,

(ii) if the distribution extends out to infinity and

if $P(u)$ is a primitive of $u\chi(u)$, then the potential V at a field point (x, y, z) is:

$V(x, y, z)$

$$= -\frac{abc}{2\varepsilon_0} \int_0^\infty \frac{P\left(\sqrt{\frac{x^2}{a^2+t}+\frac{y^2}{b^2+t}+\frac{z^2}{c^2+t}}\right)}{(a^2+t)(b^2+t)(c^2+t)} dt$$

The three components of the corresponding electric field can be derived by differentiating under the integration sign and one obtains:

$$F_x = -\chi_0 \frac{qe}{2\varepsilon_0} abcx$$

$$\cdot \int_0^\infty \frac{\exp\left[-\frac{1}{2}\left(\frac{x^2}{a^2+t}+\frac{y^2}{b^2+t}+\frac{z^2}{c^2+t}\right)\right]}{(a^2+t)\sqrt{(a^2+t)(b^2+t)(c^2+t)}} dt$$

and analogous expressions for F_y and F_z, where:

$$q = \frac{I}{4Nf}$$

is the supercharge carried by superparticles (cf. Sec. 3.1).

The three components of the force are evaluated, at each step, for all the N particles using Gauss' numerical integration method with ten points. This has proved to be a fair approximation (better than 1 per cent) in most practical cases.

According to this method the integral:

$$I = \int_a^b \phi(t') dt'$$

can be approached by:

$$I = \frac{b-a}{2}[H_1 \phi(t_1')+\ldots+H_{10} \phi(t'_{10})],$$

where

$$t_i' = \frac{a+b}{2}+\frac{b-a}{2}u_i,$$

the u_i's are the roots of the Legendre polynomial of degree ten and:

$$H_i = \int_{-1}^{+1} \frac{\prod\limits_{s\neq i}^{n}(u-u_s)}{\prod\limits_{s\neq i}^{n}(u_i-u_s)} du.$$

The integration limits of the force integral can be conveniently transformed into 0 and 1 by changing the independent variable according to the equation:

$$t = \frac{1}{t'}-1.$$

Then

$$I = \int_0^\infty f(t) dt$$

becomes

$$I = \sum_{i=1}^{10} W_i f(t_i),$$

where $W_i = H_i/2t_i'^2$ and f, for the x-component of the force, is

$$f(t) = \frac{1}{2}\frac{\exp\left[-\frac{1}{2}\left(\frac{x^2}{a^2+t}+\frac{y^2}{b^2+t}+\frac{z^2}{c^2+t}\right)\right]}{(a^2+t)\sqrt{(a^2+t)(b^2+t)(c^2+t)}}$$

The computer Central Memory storage required by MAPRO 2 is approximately 170 000 (octal) words, for a maximum of 5000 super-particles.

The CDC 6600 CPU time needed to compute one complete interaction of 500 particles turns out to be $\simeq 1$ sec which compares with the 7.5 sec of MAPRO 1 for a similar computation. For example, MAPRO 2 traces 500 particles through the CERN linac tank 1, 42 cells, i.e. 84 space-charge computations, in about 1.5 min. Taking 5000 particles instead of 500 increases the computing time up to 12 min.

4. RESULTS

4.1. Initial Results

The aim of the first computations made with MAPRO 1 and MAPRO 2 was essentially to confirm, qualitatively at least, the results already obtained by Dr. Chasman.[1,2] These initial results have already been reported in Ref. (11): they refer to the experimental 3-MeV CERN linac,[12] which is an 18-cell AG-focusing machine (mode $+ + - -$) reproducing almost exactly the first part of the CERN PS injector (injection energy 500 keV).

The comparison with Dr. Chasman's calculations can therefore be only an approximate one since her results refer to the AGS injector (input energy 750 keV).

In the computations the quadrupole gradients have been kept to their theoretical zero current

values. The initial filling was the same as used by Dr. Chasman namely a uniform filling of a four-dimensional hyperellipsoid in x, x', y, y', and of a two-dimensional ellipse in W, φ.

Figure 3 which appeared in Ref. (11), summarizes the results. One can see that:

(1) For constant nonzero current, the output radial emittance E_0 tends to coincide with E_i when E_i becomes very large: on the other side when E_i tends to zero E_0 tends towards a finite value. This confirms the results given in Ref. (1).

(2) MAPRO 2 gives emittance growths about 20 per cent larger than MAPRO 1 which can be explained by considering the different principles on which the two programs are based. The fact that MAPRO 1 tends to underevaluate space charge has already been pointed out (cf. Sec. 3.2).

(3) If one decreases the longitudinal emittance,

the radial emittance blow-up becomes less important. This also confirms results in Ref. 2.

4.2. Choice of the Injection Energy

The mechanism of the beam emittance blow-up and of the coupling between longitudinal and transverse phase spaces will not be further examined here. As explained in the Introduction, another paper, to be submitted to this journal, will be entirely dedicated to the subject (see also Ref. 13). The purpose of this paper is essentially to present the computation methods and to indicate what sort of information one can expect to extract from space-charge dynamics programs. As an exercise, the authors tried to answer the following question: what kind of output beam improvement can one obtain by increasing the injection energy into an already existing linac, with the hypothesis of simply chop-
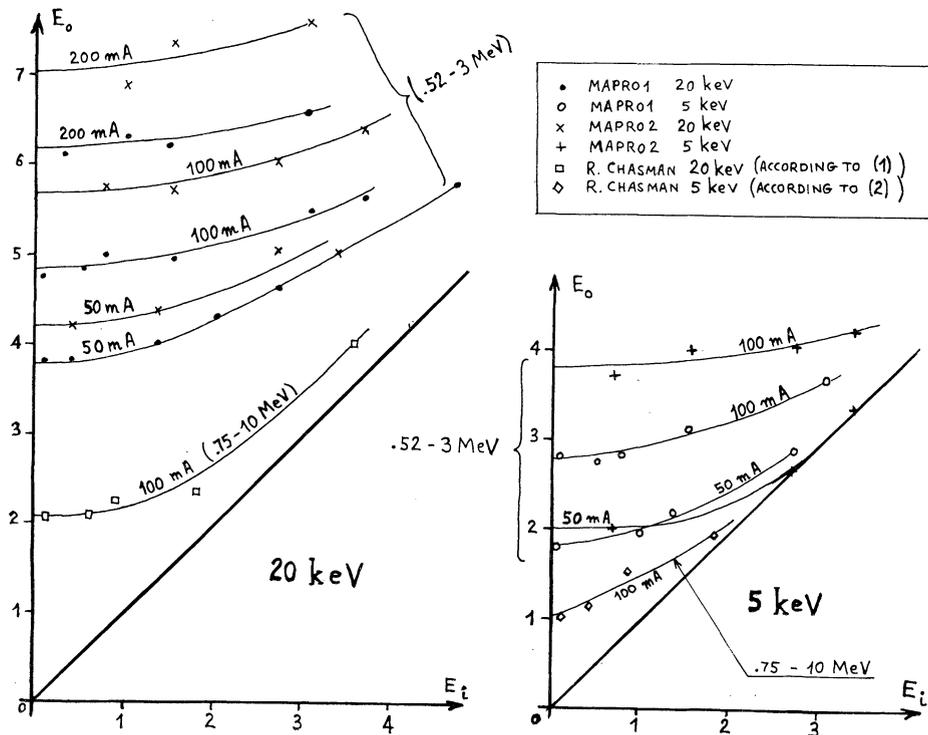

FIG. 3. Output normalized emittance E_0 versus input normalized emittance E_i; units: π 10^{-6} meter radian. For the diagram on the left a large input energy spread was chosen: 20 keV, which means an equivalent normalized longitudinal emittance:

$$\int\int \frac{d(\Delta W)\,dz}{m_0 c^2 \beta} = 2.5\ \pi 10^{-6}\ \text{m.rad}$$

for the 0.52 to 3 MeV case. For the diagram on the right a smaller input energy spread was chosen: 5 keV; corresponding longitudinal emittance is 0.5 π 10^{-6} m.rad.

ping off the first few cells? The detailed answer is given in Ref. 14: in what follows, only the main conclusions will be reproduced.

The machine considered is the CERN PS injector. The calculation was stopped at 10 MeV essentially because very little additional information was to be expected by continuing the computation beyond the first tank. Basically MAPRO 2 was used tracing in most cases 500 particles in order to save computer time. Three input current levels (200, 400 and 600 mA) have been studied for each of four possible injection energies (0.520, 0.788, 1.00 and 1.51 MeV) corresponding to suppressing the first 0, 3, 5 or 9 cells. For each of these 12 cases four focusing laws have been tried (always in the + + − − mode) by recomputing the gradients according to the formula:

$$\bar{G}_i = \alpha \beta_i^{-n} \qquad i \leq 18$$

$$\bar{G}_i = G_i \qquad i > 18$$

where β_i is v/c at cell number i, and $\bar{G}_i$ indicates the new gradient in the ith quadrupole and G_i the old one; α and n were chosen such that:

$$\bar{G}_{18} = G_{18}, \quad \bar{G}_1 = G_1 \times (1 \text{ or } 1.1 \text{ or } 1.2 \text{ or } 1.3)$$

Therefore the four cases considered corresponded to: nominal gradients (as originally calculated for zero current), 10, 20, and 30 per cent increases above nominal values.

The field level was the nominal field in the actual linac.

The initial population of the six-dimensional phase space was made according to the method described in Ref. 1. That is an uniform pseudo-random filling of a four-dimensional hyperellipsoid in x, x', y, y' and an independent random filling (also uniform) of an ellipse in longitudinal phase space.

Numerically the values used were:

$$\Delta W = \pm 20 \text{ keV}$$

and $\Delta \phi$ was chosen such as to be matched; the transverse two-dimensional emittance:

$$E_t = 22.5 \, I \pi \text{ cm mrad unnormalized}$$

with I in amperes, which corresponds at 0.520 keV to 3.34π mm mrad normalized for a 450 mA beam. One of the hypotheses of the calculation is that the source delivers a beam with an emittance linearly increasing with the current and that the preinjector deteriorates the beam quality keeping the unnormalized emittance constant between 0.52 and 1.51 MeV.

The beam x and y dimensions, for each value of E_t, were chosen such to have a nicely matched beam.

The output current as a function of input current for various injection energy levels is displayed in Fig. 4. All of these curves have been drawn using only best cases, i.e. optimized with respect to quadrupole field levels. Normally, the highest output current was obtained by increasing the first quadrupole by some 20 per cent and recomputing the others as explained above.
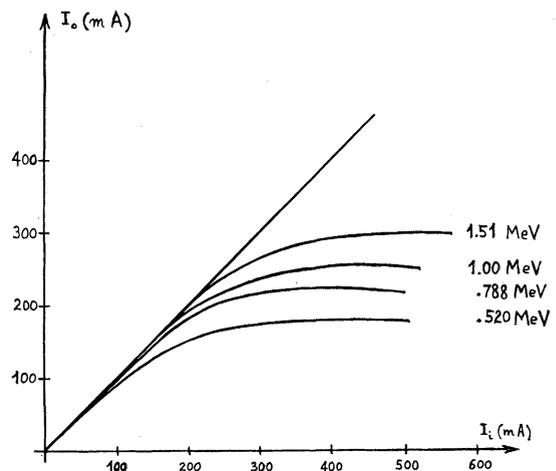

FIG. 4. Output current I_0 at 10 MeV as a function of input current I_i for various injection energies.

As can be seen, the influence of increasing the injection energy on the output current depends strongly on the input current level: up to ∼ 200 mA one has a noticeable gain passing from 0.52 to 0.788 MeV but not much improvement is to be expected by injecting at higher energy (essentially because one is very close to the limiting value). At the other extreme for 600 mA injected, the output current keeps on increasing roughly linearly with the injection energy. To estimate what sort of input current one can expect to accelerate, it must be kept in mind that the input current used in the initial filling, is made up of protons all falling longitudinally within, say, ±30 degrees from synchronous phase and ±20 keV from synchronous

energy. A rough way of evaluating what percentage this represents of the total unbunched current gives a value of 50 per cent (the buncher factor with high current is <0.6 and another factor 0.9 is needed to obtain the current within the required phase and energy intervals).[15] Also, when using Fig. 4, it must not be forgotten that the output currents are optimistic by some 20 per cent.† Let us try to clarify the importance of these two points with an example.

Suppose one expects to be able to accelerate 600 mA through the column and wants to know what energy one should aim at to obtain 200 mA of 10-MeV current. Looking at Fig. 3 corresponding to $I_0 = 240$ mA ($200 + 20$ per cent) and of $I_i = 300$ mA (50 per cent of 600) one finds an injection energy comprised between 1 and 1.5 MeV.

Table I summarizes the results concerning beam emittance growth.

In this table all emittances are normalized and expressed in arbitrary units: their values have been calculated using the statistical method described in Ref. 1.

All of the calculations (described herein) seem to show that there is a great interest in raising the injection energy for obtaining both more output current and a better quality beam.

In particular, for relatively low levels of input current, up to say 200 mA, the gain, with increase in injection energy, in brilliance, is due more to a decrease in output emittance than to an increase in output current. The opposite is true for very intense input beams.

Two important considerations should not be forgotten when drawing conclusions from this numerical exercise:

(i) all of the calculations were based on a set of starting hypotheses to some extent arbitrary,

(ii) different solutions can be tried together with raising the injection energy to obtain better results, the most obvious being, for example, to try a $+ - + -$ focusing structure.

---

† A rough estimate of how optimistic the answer is can be deduced from a practical case. The curves given in Fig. 4 show, for example, that for 200 mA of injected current one obtains an output current of 150 mA. Experimentally, under comparable conditions, one finds, say, 120 mA, i.e. 20 per cent less.

TABLE I

Influence of Injection Energy on Output Current and Output Emittances

MeV Inj. energy	mA I_i	mA I_0	Transverse E_i	Transverse E_0	Longitudinal E_i	Longitudinal E_0
	200	152	2.5	9.8	3.5	4.1
0.520	400	177	5.1	15.4	4.3	6.1
	600	164	7.6	19.0	4.8	8.4
	200	182	3.1	9.4	2.9	4.4
0.788	400	222	6.6	13.7	3.2	5.5
	600	198	8.4	18.9	4.0	6.6
	200	193	3.5	9.4	2.6	3.9
1.00	400	252	6.8	13.7	3.2	5.3
	600	231	9.6	16.8	3.6	6.3
	200	198	4.4	5.5	2.1	3.3
1.52	400	291	8.7	14.5	2.6	4.7
	600	292	12.6	19.9	3.0	5.8

I_i = input current.
E_i = input emittance at injection energy indicated.
E_0 = output emittance at 10 MeV.

5. CONCLUSIONS

Two methods of computing space-charge effects in beam dynamics have been worked out and, correspondingly, two computer programs have been prepared.

The results obtained seem to be in reasonable agreement among themselves and with those produced independently by Dr. Chasman: this suggests that numerical techniques are trustworthy.

One of the programs used proved to be fast enough to allow one to carry out relatively long and complicated numerical experiments such as the one described in Sec. 4.

It is fair to conclude that these programs, though yielding approximate results which need some interpretation, seem to be among the few valid tools to tackle complicated problems such as the dynamics of intense current beams.

REFERENCES

1. R. Chasman, in *Proc. 1968 Proton Linear Accelerator Conference, Brookhaven National Laboratory*, J. W. Bittner, ed., BNL 50120, Part 1, 372.

2. R. Chasman, *IEEE Trans. Nucl. Sci.* **NS–16**, No. 3, 202 (1969).

3. M. Promé, "Détermination de l'accélérateur linéaire de 20 MeV, nouvel injecteur du synchrotron Saturne," Rapport CEA R–3261 (1968).

4. D. A. Swenson, D. E. Young, and B. Austin, in *Proc. 1966 Linear Accelerator Conference, Los Alamos*, LA–3609, 229.

5. B. Austin, T. Edwards, J. O'Meara, M. Palmer, D. Swenson, and D. Young, "The design of proton linear accelerators for energies up to 200 MeV," Report MURA 713 (1965), unpublished.

6. M. Martini and D. Warner, "Numerical calculations of linear accelerator cavities," Report CERN 68–11 (1968).

7. B. Schnizer, "General properties of fields and beam dynamics in a linac gap," Report CERN 69–3 (1969); see also *IEEE Trans. Nucl. Sci.* **NS–14**, No. 3, 557 (1967).

8. M. Promé and R. Vienet, "Remarques sur le coefficient d'aberration," Saclay Report SEFS TD 66/46 (1966).

9. F. Vermeulen, "Computer simulation of beam bunching with the inclusion of space charge forces and quadrupole lenses," CERN Report MPS/Int.LIN 67–5 (1967).

10. B. Houssais, private communication.

11. M. Martini and M. Promé, "Beam dynamics in a proton linac with space charge," *Proc. VIIth Intern. Conf. High Energy Accelerators, Yerevan, USSR, 1969*, p. 223.

12. E. Boltezar, H. Malthouse, and D. Warner, in *Proc. 1968 Proton Linear Accelerator Conference, Brookhaven National Laboratory*, J. W. Bittner, ed., BNL 50120, Part 2, 626.

13. J. M. Lefebvre and M. Promé, "Operation of the 20 MeV linac injector of the 3 BeV Saclay synchrotron," *Proc. 1970 Proton Linear Accelerator Conference, National Accelerator Laboratory*, p. 29.

14. M. Martini, "Computer simulation of linac beam dynamics with space charge," CERN Report MPS/LIN 69–20 (1979).

15. D. J. Warner, "Methods of controlling and reducing the energy spread of the P.L.A. output beam," P.L.A. Progress Report 1963, 16, NIRL/R/60.